

REPETITIVE PULSE ACCELERATOR TECHNOLOGY FOR LIGHT ION INERTIAL CONFINEMENT FUSION*

M. T. Buttram
Sandia National Laboratories
P. O. Box 5800
Albuquerque, NM 87185

Abstract

Successful ignition of an inertial confinement fusion (ICF) pellet is calculated to require that several megajoules of energy be deposited in the pellet's centimeter-sized shell within 10 ns. This implies a driver power of several hundreds of terawatts and power density around 100 TW/cm^2 . The Sandia ICF approach is to deposit the energy with beams of 30 MV lithium ions. The first accelerator capable of producing these beams (PBFA II, 100 TW) will be used to study beam formation and target physics on a single pulse basis. To utilize this technology for power production, repetitive pulsing at rates that may be as high as 10 Hz will be required. This paper will overview the technologies being studied for a repetitively pulsed ICF accelerator. As presently conceived, power is supplied by rotating machinery providing 16 MJ in 1 ms. The generator output is transformed to 3 MV, then switched into a pulse compression system using laser triggered spark gaps. These must be synchronized to about 1 ns. Pulse compression is performed with saturable inductor switches, the output being 40 ns, 1.5 MV pulses. These are transformed to 30 MV in a self-magnetically insulated cavity adder structure. Space charge limited ion beams are drawn from anode plasmas with electron counter streaming being magnetically inhibited. The ions are ballistically focused into the entrances of guiding discharge channels for transport to the pellet. The status of component development from the prime power to the ion source will be reviewed.

Introduction

Successful demonstration of ICF in the laboratory could lead to economic generation of electric power, but extensive engineering developments in all aspects of the reactor will be required to realize this potential. An ICF reactor would include an accelerator (the driver), a system for injecting deuterium-tritium fusion pellets, a reaction chamber to absorb the energy from the exploded pellet, and a thermal-to-electrical conversion system. The driver includes an electrical power source, a means for converting that power to a photon or an ion beam, and a system to transport the beam to the pellet. The driver must deposit several megajoules in the centimeter-size pellet within 10 ns. If this can be done, it should be possible to ignite a fusion reaction with a net energy yield. Figure 1, 2 illustrates the type of yield that might be expected as a function of targeted beam energy. The type of beam is unimportant, provided only that it deposits its energy in the outer shell of the target pellet. From Figure 1, it is clear that conservative calculations imply that at least 3 to 4 MJ should be absorbed by the target and that a reasonable gain expectation is 50 to 100. Below 3 MJ targeted the gain becomes a sensitive function of energy. This paper will use 4 MJ as its design point. At the present time the major efforts in all ICF research programs are devoted to achieving the beam power

density required to demonstrate nuclear fusion in the laboratory on a single pulse basis (1-10 pulses per day). The PBFA-II light ion beam accelerator³ under development at Sandia National Laboratories will be the first ICF facility to come on line (1986) with an output energy in the megajoule range.

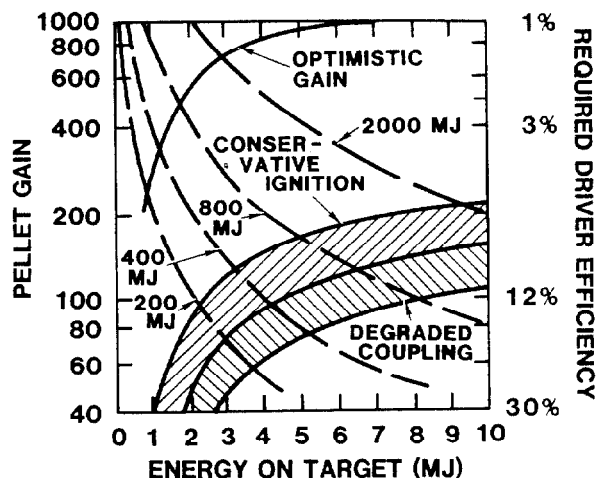


Figure 1. Pellet (target) gain as a function of energy on target for various assumptions about the coupling of the energy into the pellet. Lines of constant fusion output (energy on target times gain) are also plotted. The right vertical scale gives the driver efficiency corresponding to a given pellet gain assuming 25% recirculating power.

For reactor operation, additional requirements must be met. The driver must operate repetitively at 1 to 10 Hz. At 10 Hz, the driver must supply nearly one million pulses per day without failure and with only minor maintenance. It must be made of very reliable components which do not degrade appreciably with accumulated shots or with time on line. The driver must also be relatively efficient. For 3 MJ targeted at 10 Hz, the targeted power is 30 MW. Because of losses in the driver, some components are working at substantially higher average power. The losses are estimated to be 75%, implying that 90 MW of heat are being absorbed within the driver. This must be done nondestructively, which typically means that the heat load must be spread out. Efficiency is also coupled to reactor economics through limitations on the recirculated power. Recirculated power is that part of the reactor's output used to operate the reactor. The recirculated power must be limited to approximately 25% of the total that is generated. The product of the fraction of the power recirculated times the driver "wall plug to target" efficiency (η) times the pellet gain (Q) times the thermal to electrical conversion (thermodynamic) efficiency must be unity. Assuming a 35% thermal-electrical conversion efficiency, the product ηQ must be greater than 12. For $Q = 50$, η must exceed 20%. The efficiencies of a light ion beam driver is estimated to be 20-25% which is compatible with this requirement. (Other potential drivers, e.g. lasers, may fail at this point.)

The beam must be capable of being targeted on the pellet. Brightness, measured in $\text{TW/cm}^2/\text{rad}^2$, is a

*This work was supported by the U. S. Department of Energy under Contract No. DC-AC04-76DP00789.

measure of the ability of the driver beam to hit its target. Brightness is degraded by a number of factors including imperfections in the ion source and defocusing in flight toward the target. Data⁴ suggest that beam brightness is a strong function of voltage as shown in Figure 2. Li^+ has been chosen for PBFA-II and will be assumed for reactors because approximately 30 MV is the proper voltage to couple the energy from these ions into a pellet and should give a beam of adequate brightness.

Given that 3-4 MJ of energy from light ion beams must be delivered to the fuel pellet in 10 ns, the peak power of the beam at the target will be 300-400 TW. By controlling the temporal distribution of the ion beam voltage, it should be possible to bunch the beam, that is, to compress the pulse duration. A factor of four is projected to be possible while the beam is being transported between the accelerator and target. If we assume 50% efficiency for generating and transporting the beam to the target, the electrical power pulse must be 150 to 200 TW with a 40 ns pulse duration. It does not appear to be feasible to produce these exceptionally

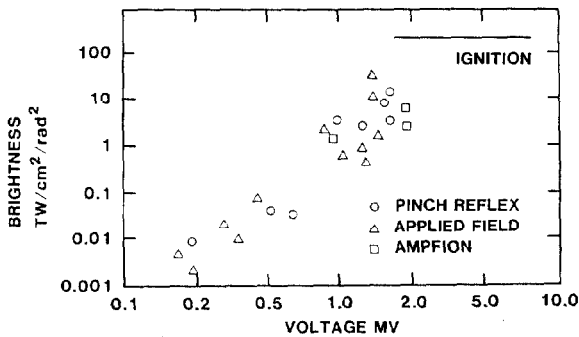


Figure 2. Experimental ion diode beam brightness as a function of accelerator voltage.

high peak powers in a single pulsed power system. Thus, the pulsed power system will be divided into several modules. PBFA-II, for example, will have thirty-six, 3-4 TW modules.³ Since the number of beam penetration points into the reactor chamber should be minimized, this paper will consider the design of modules that generate 10 TW electrical pulses. Up to 20 such modules operating in parallel would be required for a reactor.

Description of the Driver

Generically, the driver consists of an energy accumulator, a control switch which begins the pulse compression cycle, a transformer to get to a high voltage (~ 3 MV), some high speed switching to compress the pulse to 40 ns, and a final stage transformer to raise the voltage to 30 MV. The low voltage section of one 10 TW module is illustrated schematically in Figure 3. The accumulator is a rotating machine (modified alternator) configured to output 800 kJ at 30 to 50 kV in 1 ms. (This is shown as four separate symbols in the figure.) Energy is extracted from the alternator by shorting it through a transformer into C_1 using a triggered control switch. The energy stored in C_1 discharges in ~ 1 μ s through the laser triggered spark gap switch. Capacitor-saturable inductor pairs (L_2, C_2), (L_3, C_3), (L_4 , pulse forming line [PFL]) then compress the pulse to a 40 ns, 1.5 MV, 2 MA, 3 TW output. Four such lines feed the final adder system.

Figure 4 is an artist's conception of a single module. The four pulse compression lines are combined beyond saturable inductor L_4 into two feed lines, on one either side of the HV transformer. The pulses from these lines are split into 20 equal (1.5 MV) parts, then added in the induction cavities. Table I gives the estimated energy efficiency for each element in the pulsed power system. The transformer, spark gap switch, and saturable inductor efficiencies are extrapolated from existing data. The splitter and cavity efficiencies are estimates. The adder efficiency will be discussed later. The primary points to be made by the table are that the loss per component is small but the overall efficiency is still 50% and that the losses are distributed and therefore tolerable.

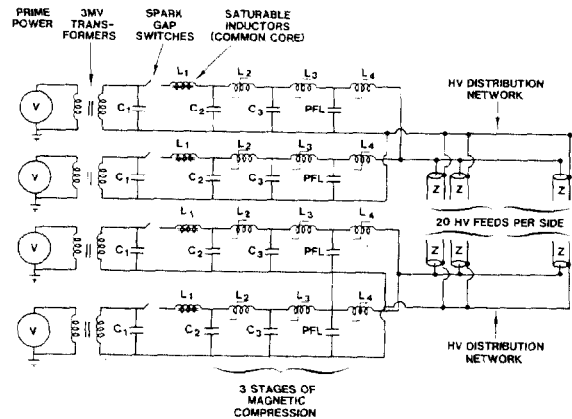


Figure 3. Electrical schematic of the pulse compression section of one 10 TW module.

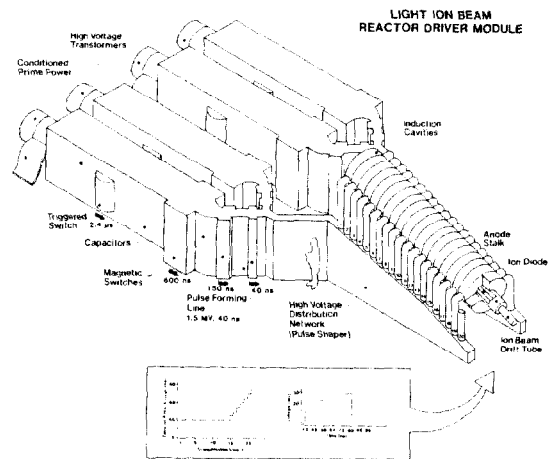


Figure 4. Artist concept of a 10 TW module. Insert shows the output electrical pulse.

Table I. System Efficiencies

Element	Estimated Efficiency
Adder	88%
Single Cavity	90%
Splitter	90%
L_4	95%
L_3	95%
L_2	95%
Spark Gap Switch	90%
Transformer	90%
Net	48%

The alternator is being prototyped at present at the 10 KV, 20 kJ level. The initial design is a 500 Hz alternator configured with minimal internal impedance to maximize the surge output upon closure of the control switch. Generically the output will be a fully offset 500 Hz sine wave. The current rises from zero at $t = 0$ and dips just below zero at 1 ms. Peak current is about 1 kA for 20 kJ output. The control switch will be SCR array that will take advantage of the current reversal to open and limit the alternator discharge to the first pulse. Megajoule outputs and gigawatt instantaneous power are projected to be feasible.

The capacitor C_1 will provide 3 MV, millisecond energy storage. Options are a series of conventional foil capacitors or a chilled (-35°C) water-ethylene glycol device. Water-glycol mixtures have been studied for millisecond energy storage by several authors.⁵ The work needs to be extended to higher voltage and higher stored energy. Pulse transformers have been operated to 3 MV single shot and to 1.5 MV at 15 Hz⁶. Again, the total energy needs to be increased.

The decision to transform directly to 30 MV is based on the requirements for the spark gap switch. It will charge in ~ 1 ms and discharge in ~ 1 μs . A gas spark gap, and nothing else, can perform this service at 10 Hz. This system was designed to minimize the utilization of spark gap switches, but there seems to be little likelihood of avoiding them altogether. Nor is there any need to do so. They are reliable in this type of service although prudence suggests limiting their number. An alternative to this design is to charge C_1 to the alternator output voltage, then discharge through a transformer in about a microsecond to charge C_2 to 3 MV. Effectively, the difference between this and the preferred scenario is that in the preferred case, the spark gap operates at high voltage, low current, and in the other case, it works at low voltage, high current. Spark gaps tend to become unstable in repetitive service as a result of surface damage above 100 kA. The number of spark gaps, then, is controlled by the limitation of total current to 100 kA per switch. To a reasonable approximation, the energy U transferred through a spark gap is $U = VIt$, where V is the voltage across the gap prior to closure, I is the spark gap current, and t is the discharge time. In the preferred scenario $V = 3$ MV, while in the alternate $V = 50$ kV. Assuming $t = 1$ μs and $U = 1$ MJ, the currents for the two scenarios are 330 kA and 20 MA. The preferred scenario requires four spark gaps, the alternate 200 per megajoule. Effectively, one trades a multiple spark gap problem for an insulation problem (3 MV vs. 50 kV). The latter is thought to be more tractable. The major problem may be to ensure nanosecond synchronization in the closure of the spark gap switches in either scheme. This has been achieved at 5 MV on a single pulse basis using UV laser triggering (Figure 5).⁷ We anticipate that an equivalent will suffice at 10 Hz and are beginning experiments to demonstrate a 2 to 3 MV device.

Once any spark gap closes, the pulse compression sequence for that section of the module proceeds to the generation of an output pulse. There is no provision to abort in case of a spark gap prefire because the remainder of the pulse compression sequence uses saturable inductors. Figure 6 is an illustration of a saturable inductor mounted in an enclosed triplate line. The inductor blocks power flow through the line because of its high unsaturated

inductance. Thus, the left-hand (near) side of the line may be charged with little leakage beyond the inductor. As the voltage across the inductor builds up, its leakage current builds up until the ferromagnetic material saturates. For a properly designed system, the energy can then flow out through the inductor much faster than it was stored originally. Power gains of 3 to 4 are practical and the final output power can be substantial. Figure 7 shows a 2.7 MV, 3 TW pulse generated with saturable inductor switching.⁸ Inductor switches are very low loss and appear to have no lifetime or repetition rate limits in the range of interest of this work.⁹ Thus they are ideal for the ICF reactor application.

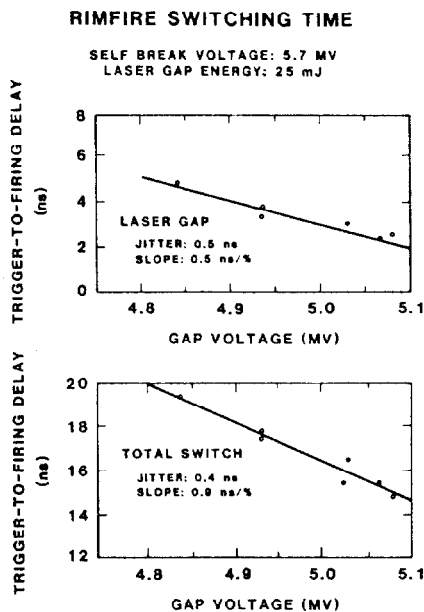


Figure 5. Trigger to firing delay for a multiple stage switch. The first stage is laser triggered (upper plot). The remainder of the switch self-fires (lower plot).

The shape of the output pulse is determined by the final PFL and saturable core. Saturation occurs when Eq. 1 is satisfied.

$$\int_0^T V dt = A \Delta B \quad (1)$$

where V is the voltage across L_4 , A is the cross-sectional area of its magnetic material and ΔB is the flux swing in the core material between its initial state and saturation. For a $V_0 (1 - \cos \omega t)$ charging waveform on the PFL, switching at peak voltage (time T) corresponds to

$$\int_0^T V dt = V_0 T/2 \quad (2)$$

The rise time of the final pulse may be limited by the inductance of the switch. For a typical geometry like the strip line of Figure 6, the contribution to the output pulse rise time will be

$$\tau_{\text{RISE}} = 2.2 L_{\text{SAT}}^{1/2} \\ = 1.1 \mu\text{A}^{1/2} / WZ \quad (3)$$

where τ is the 10% to 90% rise time of the pulse, μ is the permeability of the core after saturation, A' is the total cross sectional area of the core (including the insulation between the saturable ferromagnetic strip windings), W is the total length around the core in the direction of the magnetic field, and Z is the common impedance of the PFL and output transmission lines.

The area A' in Eq. 3 is larger than A in Eq. 1 by a packing factor F because A' contains the area required for core electrical insulation. Eliminating the area terms from Eq. 1, 2, and 3 gives

$$\tau_{RISE} = \frac{1.1 \mu_0}{\Delta B} \frac{IT F}{W} \tag{4}$$

$$= 4.3 \times 10^{-7} (IT F/W) \tag{5}$$

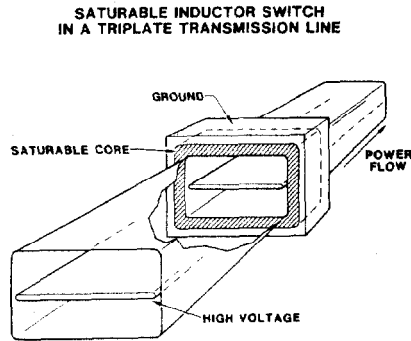


Figure 6. Sketch of two triplate transmission lines (impedance Z) connected by a magnetic switch.

EXPERIMENTAL RESULTS AGREE WITH SCEPTRE SIMULATION

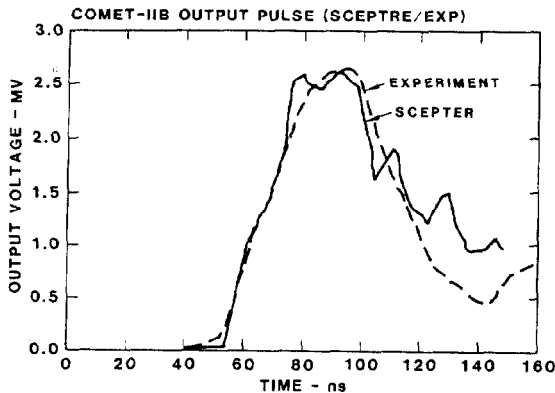


Figure 7. Magnetic switch output (2.7 MV) compared to circuit model (SCEPTRE) calculation.

$I = V_0/2Z$ is the output current. Metglas cores¹⁰ ($\Delta B = 3.2$ T) are assumed.

The transmission lines on either side of the magnetic switches would be an enclosed triplate design of the type shown in Figure 6. The dielectric is water (dielectric constant 81). Allowable working stresses for water in single pulse operation are known, but the equivalent levels for reliable, long life operation are not accurately known. Derating the single pulse data gives a reasonable estimate of 200 kV/cm. Then the spacing d in the PFL at 3 MV must be 15 cm. The PFL impedance (ignoring end effects) is

$$Z = 0.81 \Omega = \frac{377}{\sqrt{81}} \frac{d}{W} \tag{6}$$

giving $W = 7.5$ m. Using Eq. 5 with $I = 2$ MA, $F = 1.2$ and $T = 1.5 \times 10^{-7}$ sec, $\tau_{RISE} = 20$ ns. This design may be a bit optimistic. An additional stage of pulse compression may well be required to form the final pulse. Nevertheless, this final rise time estimate appears to be reasonable.

Final pulse voltage amplification uses a series of cylindrical cavities of the type shown in Figure 8.

Power is fed in from one of the 20 lines from the splitter of Figure 4. It is prevented from flowing down the right side of the cavity by a high permeability magnetic coil.

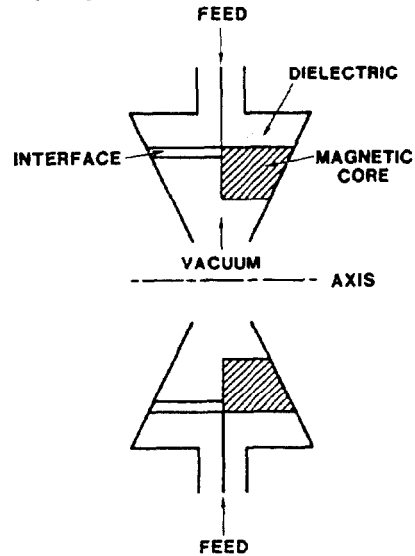


Figure 8. Cross section a cylindrical inductively-isolated acceleration cavity.

To prevent saturation of the core, its area must exceed 200 cm². The cavities feed a common diode as illustrated in Figure 9. In such a configuration, a pulse V arriving at the gap of cavity N ($1 < N < 20$) in coincidence with a pulse of amplitude $(N - 1)V$ proceeding from left to right in the diode will result in a pulse of voltage NV travelling to the right in the diode. Ideally, no pulses are reflected. Each cavity must be fed at the correct time to allow for propagation delay through earlier cavities, resulting in increasing cable lengths to the later cavities.

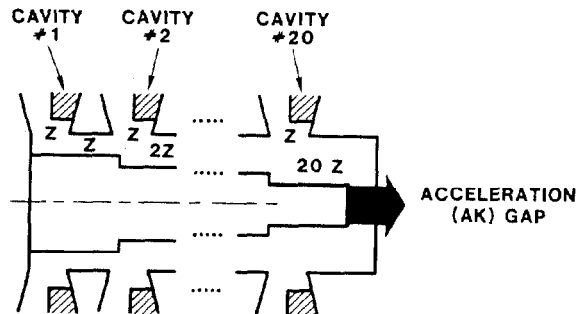


Figure 9. Schematic of 20 cavities delivering power to a common load (diode).

If a pulse does not arrive in a particular cavity ($N + 1$), the wave in the diode transmits a voltage wave of amplitude V into the cavity and the wave along the axis continues to have amplitude NV. This can be useful for shaping the output pulse. As an example, consider the insert to Figure 4. Thirteen of the 20 cavities are properly timed. Cavities 14 through 20 are pulsed late. Cavity 14 is delayed by 5 ns, cavity 15 by 10 ns ... cavity 20 by 35 ns. As each cavity pulse arrives, the output pulse increases one unit of voltage (1.5 MV) slowly ramping from 20 MV to 30 MV. This ramp is used to bunch the ions between the diode and pellet, those accelerated late in the pulse at high voltage catching the earlier low voltage ions, increasing the power on target. Any pulse shape from a square pulse to a triangle can be achieved by proper choice of the lengths of the feed cables.

Actually this scheme can be improved upon by not feeding those cavities that begin to pulse half way through the pulse or later. If those cavities are shorted and the radius properly set, the 1.5 MV pulse induced in the cavity reflects and returns to the cavity terminal producing the voltage increment at the proper time. This is only possible for cavities that should contribute half way through the main pulse or later. Any attempt to use this scheme on the first half of the pulse results in undesirable multiple reflections in those cavities.

Assuming a perfect diode of constant impedance Z , a pulse that ramps from V_1 to V_2 over time T usefully deposits

$$U_{DEP} = \frac{T}{3Z} (V_2^2 + V_1 V_2 + V_1^2). \quad (7)$$

The energy arriving at the 20 cavities is

$$U_{input} = 20 * (V_2/20)^2 T / (Z/20) \\ = \frac{V_2^2 T}{Z} \quad (8)$$

The efficiency η_c is

$$\eta_c = \frac{U_{DEP}}{U_{input}} = 1/3 \left(1 + \frac{V_1}{V_2} + \frac{V_1^2}{V_2^2} \right). \quad (9)$$

For the case illustrated in Figure 4 insert, $V_1/V_2 = 0.67$ and the efficiency is 71%. If four of the cavities are shorted, then the energy actually supplied by the pulsed power system is reduced by one fifth. The efficiency is increased correspondingly to 88%.

This adder concept was originally developed by Kerst and Brower. It forms the basis for the 2.5 MV, 70 ns ATA injector.¹² It has been extended to 4 MV, 250 kA in the HELIA¹³ program. Figure 10 is HELIA data illustrating at least 90% adder voltage efficiency in a 30 ns FWHM pulse. An extension to 30 MV will require extensive study of vacuum current flow and of pulse fidelity.

Initial half voltage tests on HELIA are promising.

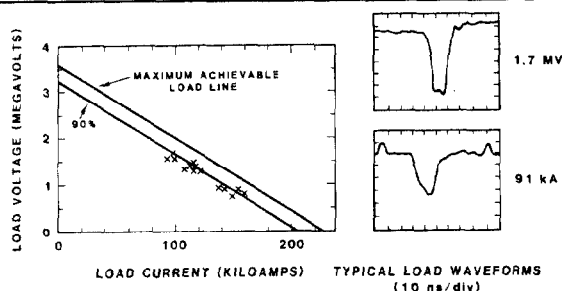


Figure 10. Waveforms and load line for the HELIA times 4 inductive voltage adder.

Conclusion

The successful operation of an ICF reactor will require extensive technological development, but recent developments have greatly enhanced the prospects for ultimate success. This paper has dealt with the pulsed power driver aspects of the program, discussing both the current state of the art and some new ideas that promise to make ICF pulsed power modules simpler and more reliable than earlier designs. Any ICF scheme would need to deliver 300 to

400 TW beams to a target pellet in a 10 ns pulse (3 to 4 MJ). Light ion power probably can be increased by a factor of four by pulse compression bunching between the source (diode) and target. Thus, the pulsed power system must deliver a shaped 40 ns pulse with peak power near 150 to 200 TW, allowing for a 50% efficiency for conversion to ions and transport to the target.

High powers and energies lead to a proliferation of pulsed power components, which raises significant questions about lifetime and reliability. This paper has presented a conceptual driver that is very simple relative to previous designs. It consists of 15 to 20 parallel modules. Each module needs four spark gaps. The remainder of the pulse compression is done with saturable inductors.

Uncertainties exist in the design of the beam source or ions. These are being partially resolved in single pulse experiments ongoing at the present time. It appears that reliable pulsed power systems for repetitive (1 to 10 Hz) beam source experiments could be developed using the concept discussed above. This would open the way for significant progress in the development of a commercial reactor.

Acknowledgement

This driver^{14,15} was designed in cooperation with K. R. Prestwich. Data on alternators were provided by D. Scott of Westinghouse Electric Corporation.

References

1. J. A. Blink, Heavy Ion Fusion Beam Transport Workshop, Los Alamos National Laboratory, Aug. 26-27, 1980.
2. D. L. Cook et al., Proceedings of the Fourth Topical Mtg. on the Technology of Controlled Nuclear Fusion, Vol. III, October 14-17, 1980, King of Prussia, PA, p. 1386.
3. G. Yonas, Proc. of U. S. - Japan Seminar on Theory and Application of Multiple Ionized Plasmas Produced by Laser and Particle Beams, May 3-7, 1982, Nara, Japan.
4. D. L. Cook, Proc., 4th IEEE Pulsed Power Conference, Albuquerque, NM, June 1983.
5. G. Yonas and J. P. VanDevencer, 6th Intl. Workshop on Laser Interaction and Related Plasma Phenomena, Monterey, CA, October 27, 1982.
6. F. J. Zutavern, M. T. Buttram, M. O'Malley, Proc. 1984 Power Modulator Symp., Alexandria, VA, p. 273.
7. D. B. Fenneman and R. J. Gripshover, IEEE Conference on Elect. Ins. and Dielectric Phenomena, New York, NY 1980.
8. G. J. Rohwein, 2nd Intl. Pulsed Power Conference, Lubbock, TX, June 1979, p. 81.
9. J. R. Woodworth, C. A. Frost, and T. A. Green, 3rd IEEE Pulsed Power Conference, Albuquerque, NM, June 1981, p. 154.
10. E. L. Neau, T. L. Woolston and K. J. Penn, Proc. 1984 Power Mod. Symp., Alexandria, VA, p. 292.
11. D. L. Birx, et. al., Proc. 1984 Power Modulator Symposium, Alexandria, VA, p. 186.
12. Metglas is an Allied Chemical Company Tradename for metallic glass (amorphous) ferromagnetic material.
13. D. W. Kerst and D. F. Brower, U. S. Patent 2976444, March 1961.
14. Ross E. Hester, et. al., IEEE Trans. on Nuclear Science, Vol. NS-26, No. 3, June 1979, p. 4180.
15. D. E. Hasti, et. al., Proc. 1984 Power Modulator Symposium., Alexandria, VA, p. 299.
16. K. R. Prestwich and M. T. Buttram, Proc. of the Fifth Topical Meeting on Fusion Tech., Knoxville, TN, April 1983
17. M. T. Buttram, et. al., Proc. Fusion Engineering Symposium, Philadelphia, PA, December 1983.